International Journal of Neuropsychopharmacology (2014), **17**, 1129–1138. © CINP 2014
doi:10.1017/S1461145714000042

ARTICLE

Changes in brain functional connectivity after chronic haloperidol in rats: a network analysis

Anne L Wheeler[1,2]*, Meaghan C Creed[3,4]*, Aristotle N Voineskos[1,2,5] and José N Nobrega[1,2,3,4,6]

[1] *Research Imaging Centre, Centre for Addiction and Mental Health, Canada*
[2] *Department of Psychiatry, University of Toronto, Canada*
[3] *Behavioural Neurobiology Laboratory, Campbell Family Mental Health Research Institute, Center for Addiction and Mental Health, Canada*
[4] *Department of Pharmacology and Toxicology, University of Toronto, Canada*
[5] *Institute of Medical Science, University of Toronto, Canada*
[6] *Department of Psychology, University of Toronto, Canada*

Abstract

Although the effects of haloperidol (HAL) have been extensively examined in experimental animals at the cellular and brain regional levels, the effects of prolonged HAL treatment on functional connectivity in the brain have not yet been addressed. Here we used expression of the immediate early gene *zif 268* as a marker of neural activity to examine changes in brain regional interactivity after 12 wk of HAL treatment in rats. *zif 268* expression was measured by *in situ* hybridization in 83 brain regions of HAL- and vehicle (VEH)-treated controls and correlations among all brain regions were computed separately for the two treatment groups. The strongest correlations in each group were used for network construction. It was found that VEH and HAL networks were equally segregated and integrated, and that both networks display small world organization. Compared to the VEH network, the HAL network showed enhanced interactivity between the dorsolateral striatum and thalamus, and between different subdivisions of the thalamus. It will be of interest to determine the extent to which the observed changes in functional connectivity may be related to dyskinesias, to changes in motivated behaviours and/or to the therapeutic effects of chronic HAL. By identifying the connectivity features of a chronic HAL network in the absence of other manipulations, the current findings may provide a reference signature pattern to be targeted in future efforts to discriminate between the neural bases of different behavioural outcomes arising from chronic HAL treatment.

Received 4 September 2013; Reviewed 20 December 2013; Revised 11 January 2014; Accepted 13 January 2014; First published online 14 February 2014

Key words: erg-1, functional connectivity, graph theory analysis, haloperidol, krox-24, network analysis, tardive dyskinesia.

Introduction

Long-term treatment with first generation antipsychotic drugs such as haloperidol (HAL) is associated with morphological and synaptic changes in the brain (Benes et al., 1985a, b), which are thought to be involved in both the therapeutic effects of HAL as well as its persistent adverse motor effects (Konradi and Heckers, 2001; Teo et al., 2012). It has been generally hypothesized that neuroplastic changes induced by classical antipsychotic drugs may promote functional and anatomical reorganization of neural connections (Eastwood et al., 1997, 2000; Harrison, 1999; Konradi and Heckers, 2001).

More recently a number of brain-wide imaging studies have also addressed morphological and functional changes induced by chronic HAL and other antipsychotic drugs in human subjects (Ebdrup et al., 2013; Roder et al., 2013). Valuable as they are, human imaging studies face the difficulty of separating medication effects from effects associated with the disease condition itself. This difficulty is avoided in experimental animals, where chronic HAL treatment has been found to induce morphological and structural changes (Benes et al., 1985a, b; Roberts et al., 1995; Kelley et al., 1997; Chakos et al., 1998; Roberts and Lapidus, 2003; Vernon et al., 2011, 2012) as well as alterations in brain-wide markers of functional activity such as 2-deoxyglucose uptake (Pizzolato et al., 1985a, b), c-Fos (Sun et al., 1998) or *zif 268* expression levels (Creed et al., 2012).

One common feature of brain mapping studies addressing the effects of chronic HAL has been a focus on localized regional changes, with much less consideration given to potential changes in interrelations among brain regions. Yet, it is commonly recognized that changes in localized brain activity may affect activity in other areas in a number of direct and indirect ways. In recent years

Address for correspondence: Dr J. N. Nobrega, Centre for Addiction and Mental Health, 250 College Street, Toronto, ON, M5T 1R8, Canada.
Tel.: +1 416 535 8501 x6259 *Fax*: +1 416 979 4739
Email: jose.nobrega@camh.ca
* Contributed equally to the work.

analytical techniques have been developed to interrogate the functional relationships between a large number of brain regions. For example, Gass et al. (2013) recently described HAL-induced functional connectivity changes using BOLD fMRI in rats. In that study, however, network analyses were conducted after an acute HAL exposure in anesthetized rats (Gass et al., 2013). In the present study we used interactivity analysis (Wheeler et al., 2013) to ascertain whether long-term HAL treatment leads to functional connectivity changes in rat brain using *zif 268* mRNA expression as a functional mapping tool. *zif 268* is an immediate early gene that is sensitive to intracellular calcium levels and alterations in neuronal firing and is commonly used as an indicator of local brain activity (Farivar et al., 2004). The *zif 268* signal is readily quantified in *in situ* hybridization autoradiograms at the brain regional level, allowing for measurements of dozens of brain regions and subregions.

Experimental procedures

Subjects and HAL treatment

Male Sprague–Dawley rats initially weighing 200–250 g (Charles River, Canada) were used for all experiments. All procedures were approved by the Animal Care Committee at the Centre for Addiction and Mental Health and complied with Canadian Council on Animal Care (CCAC) and NIH standards and guidelines.

After 1 wk acclimation to the housing facility, rats were randomly assigned to receive either haloperidol decanoate (HAL; 21 mg/kg i.m. $N=6$) or sesame oil vehicle (VEH; $N=6$) once every 3 wk for 12 wk (a total of four injections). The decanoate formulation is known to result in constant plasma HAL levels in the 1.1–1.5 mg/kg range (Turrone et al., 2002). Our intent was to use a HAL dosing regimen that would be relevant both for the beneficial therapeutic effects of the drug and for its long-term deleterious motor side effects. In rats the chosen HAL dose provides clear effects in various models of antipsychotic activity as well as models of tardive dyskinetic effects.

In situ *hybridization and densitometric analyses*

Hybridization was performed using ^{35}S-UTP labelled riboprobes complementary to *zif 268* according to Genbank # NM_012551, (bases 660–679), 5′- tcacctatactggccgcttc-3′ and (bases 1062–1043) 5′- aggtctccctgttgttgtgg-3′ and consensus promoter sequences for either SP6 RNA polymerase. Using the NCBI BLAST Tool, the sequences were checked for homology with the rat genome and found to be specific for their respective transcripts. Probes were diluted to a concentration of 200000 cpm/μl in hybridization solution containing: 50% formamide, 35% Denhardt's solution, 10% dextran sulphate, 0.1×SSC, salmon sperm DNA (300 μg/ml), yeast tRNA (100 μg/ml), and DTT (40 μM). Slides were incubated in plastic mailers overnight at 60 °C. After hybridization, sections were rinsed in 4×SSC at 60 °C, treated in RNase A (20 μg/ml) solution at 45 °C for 40 min, washed with agitation in decreasing concentrations of SSC containing 5 g/l sodium thiosulfate, dipped in water, dehydrated in 70% ethanol, and air-dried. The slides were exposed to Kodak BioMax film for 6 d at 4 °C along with calibrated radioactivity standards. Probe specificity was confirmed by testing labelled sense and scrambled probes, both of which produced no measurable signal on film.

Densitometric analyses were performed with MCID 7.0 software (InterFocus, Linton, UK). Prior to sampling, illumination level was adjusted for every film to ensure consistent background readings across all films. Standard curves obtained from calibrated radioactivity standards were used to convert raw optical density values to radioactivity levels in microcuries per gram of tissue (μCi/g). These values were determined in 83 distinct regions of the rat brain (Table 1). Regions were defined according to the atlas of Paxinos and Watson (Paxinos and Watson, 1986) with no *a priori* selection of regions of interest. Thus the only criterion for inclusion of brain regions was clear definition on film. Densitometric readings were performed in 36 stions per brain by an operator who was blind to group treatment. Measurements were first averaged across all sampling windows for each section and then across all sections to produce a final density value for each region for each brain. Representative pictomicrographs illustrating regional *zif 268* expression in VEH and HAL brains are shown in Fig. 1.

Interactivity analysis

Correlation matrices

Using the *zif 268* signal as a dependent variable, all possible pairwise correlations between the 83 brain regions were computed using Pearson correlation coefficients in HAL and VEH groups separately, totalling 3403 correlations for each group. Each complete set of correlations was displayed as colour-coded correlation matrices using Matlab software (Mathworks Inc., USA). Correlation matrices for HAL and VEH groups were then compared, with all individual correlations initially included (Fig. 2*a, b*). Significant differences in individual correlations were then determined using permutation testing. This involved randomly shuffling subject group labels to produce a large number of random groupings from the two original sets of data. Following each permutation the test statistic (correlation coefficient) was recalculated; a sampling distribution was generated and the probability of the number of observed events being greater than the number expected by chance was computed. In addition, the false discovery rate (Benjamini and Rochberg, 1995; Genovese et al., 2002) was controlled at the 5% level, given the number of multiple comparisons. The entire procedure was repeated using

Table 1. Brain region abbreviations

Abbreviation	Brain region	Bregma[a]	Region #
Thalamus			
Thal PVA	Paraventricular thalamic n.	−3.30	1
Thal PT	Parataenial thalamic n.	−2.10	2
Thal PC	Paracentral thalamic n	−3.30	3
Thal AV	Anteroventral thalamic n.	−2.10	4
Thal AD	Anterodorsal thalamic n.	−2.10	5
Thal AM	Anteromedial thalamic n.	−2.10	6
Thal Re	Reuniens thalamic n.	−3.00	7
Thal Rh	Rhomboid thalamic n.	−3.00	8
Thal CM	Centromedian thalamic n.	−3.30	9
Thal VL	Ventrolateral thalamic n.	−3.00	10
Thal VM	Ventromedial thalamic n.	−3.30	11
Thal MD	Mediodorsal thalamic n.	−3.30	12
Thal VP	Ventroposterior thalamic n.	−3.80	13
Thal LDDM	Laterodorsal n.,dorsomedial	−3.30	14
Thal LDVL	Laterodorsal n., ventrolateral	−3.30	15
Thal Po	Posterior thalamic n.	−4.50	16
LHb	Lateral habenular n.	−3.60	17
LHb-E	Lateral habenula, external	−3.60	18
MHB	Medial habenular n.	−3.60	19
Hypothalamus			
Hypo PaV	Paraventricular hypothalamic n.	−1.80	20
Hypo LH	Lateral hypothalamic area	−3.14	21
Hypo AHC	Anterior hypothalamic area, central	−2.10	22
Hypo Arc	Hypothalamic arcuate n.	−3.60	23
Hypo VMH	Ventromedial hypothalamic n.	−3.60	24
Hypo DMD	Diffuse dorsomedial hypothalamic n.	−3.60	25
Midbrain			
MRN	Median raphe n.	−8.00	26
VTA	Ventral tegmental area	−6.50	27
PPTg	Pedunculopontine tegmental n.	−8.00	28
DRN	Dorsal raphe n.	−8.00	29
Basal ganglia			
Post CPu	Posterior caudate putamen	−2.10	30
Ant CPu	Anterior caudate putamen	1.70	31
DL CPu	Dorsolateral caudate putamen	−0.26	32
DM CPu	Dorsomedial caudate putamen	−0.26	33
VL CPu	Ventrolateral caudate putamen	−0.26	34
VM CPu	Ventromedial caudate putamen	−0.26	35
GPe	External globus pallidus	−1.30	36
EPN	Entopeduncular n.	−3.00	37
SNr	Substantia nigra pars reticulata	−5.80	38
SNc	Substantia nigra pars compacta	−5.80	39
STN	Subthalamic n.	−4.20	40
Cortex			
Post Pir	Posterior piriform cortex	0.00	41
Ant Pir	Anterior piriform cortex	2.20	42
Cing Crtx	Cingulate cortex	0.70	43
mPFC	Medial prefrontal cortex	2.20	44
Ent Cortex	Entorhinal cortex	−5.80	45
PRh Cortex	Perirhinal cortex	−3.30	46
Tell cortex	Temporal cortex	−7.80	47
Oc Cortex	Occipital cortex	−4.50	48
MOs	Supplementary motor cortex	0.70	49
MOp	Primary motor cortex	0.70	50
Post MOs	Posterior supplementary motor cortex	−1.40	51

Table 1. (*Cont.*)

Abbreviation	Brain region	Bregma[a]	Region #
Post MOp	Posterior primary motor cortex	−1.40	52
Fr2	Frontal cortex, area 2	1.20	53
Fr1	Frontal cortex, area 1	1.20	54
Fr3	Frontal cortex, area 3	1.20	55
Par	Parietal cortex	−4.50	56
Cerebral nuclei			
Clstrm	Claustrum	0.20	57
AntOlfNuc M	Anterior olfactory n., medial	3.70	58
AntOlfNuc V	Anterior olfactory n., ventral	3.70	59
AntOlfNuc P	Anterior olfactory n., posterior	2.70	60
IslCaj	Islands of Calleja	2.20	61
NAc Core	N. accumbens core	0.70	62
NAc Shell	N. accumbens shell	0.70	63
Acb	Anterior n. accumbens	3.20	64
VP	Ventral pallidum	−0.80	65
MS	Medial septum	−0.26	66
LS D	Lateral septum, dorsal	−0.26	67
LS V	Lateral septum, ventral	−0.26	68
LS I	Lateral septum, intermediate	−0.26	69
mfb	Medial forebrain bundle	−1.30	70
fornix	Fornix	−3.00	71
Amyg BLA	Basolateral amygdaloid n.	−2.80	72
Amyg La	Lateral amygdaloid n.	−2.80	73
Amyg BLV	Basolateral amygdaloid n., ventral	−2.80	74
Amyg BLP	Basolateral amygdaloid n., posterior	−2.80	75
Amyg BM	Basomedial amygdaloid n.	−2.80	76
Amyg PLCo	Posterolat. cortical amygdaloid area	−4.10	77
Amyg ACo	Anterior cortical amygdaloid area	−2.30	78
Hippocampus			
HC CA3	Hippocampal CA3 field	−5.80	79
HC CA1	Hippocampal CA1 field	−5.80	80
HC CA2	Hippocampal CA2 field	−5.80	81
HC CA4	Hippocampal CA4 field	−5.80	82
HC DG	Hippocampal dentate gyrus	−5.80	83

[a] Bregma reference corresponds to average anterior–posterior level (in mm) where sections were taken and analysed. In general most brain areas were analysed in 3–5 stions around this value.

Spearman's rank correlation coefficients, to ensure that correlation patterns were not driven by outliers.

Network construction

Networks were constructed by considering the strongest inter-regional correlations in each group of animals. In selecting a threshold criterion for inclusion in the network we examined a progressive series of increasing r values and the corresponding series of decreasing numbers of brain areas to be treated as nodes in the network. In an effort to balance a stringent r threshold with a reasonable number of network nodes to be included, the decision was made to retain the top 4% of the r distribution in each group. This corresponded to $r>\pm0.90$ in the HAL network and $r>\pm0.89$ in the VEH network. The nodes in the resulting networks represent brain regions and the correlations that survived the threshold criterion were considered to be functional connections. Cytoscape software (Cline et al., 2007) (http://www.cytoscape.org/) was used to visualize the resulting networks, where node colour was set proportional to degree (number of connections) and connection line weights reflect the strength of the correlation. A graphical representation of networks of inter-region relationships created using the chosen 4% criterion is shown in Fig. 3.

Analysis of network properties

Descriptions and explanations of basic network concepts are available (Dong and Horvath, 2007; Rubinov and Sporns, 2010). *Connection density*, defined as the number of connections present out of all possible connections, was calculated across a range of correlation coefficient

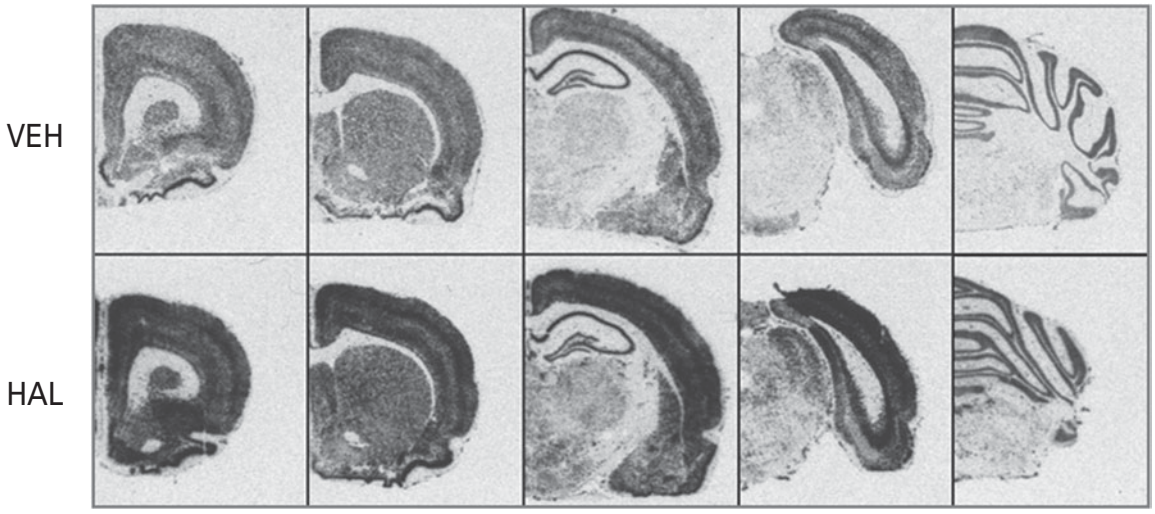

Fig. 1. *zif 268* mRNA after chronic haloperidol (HAL) treatment. Pictomicrographs illustrating the overall [^{35}S]-labelled *zif 268* mRNA expression on film at different coronal levels of vehicle and HAL rat brains.

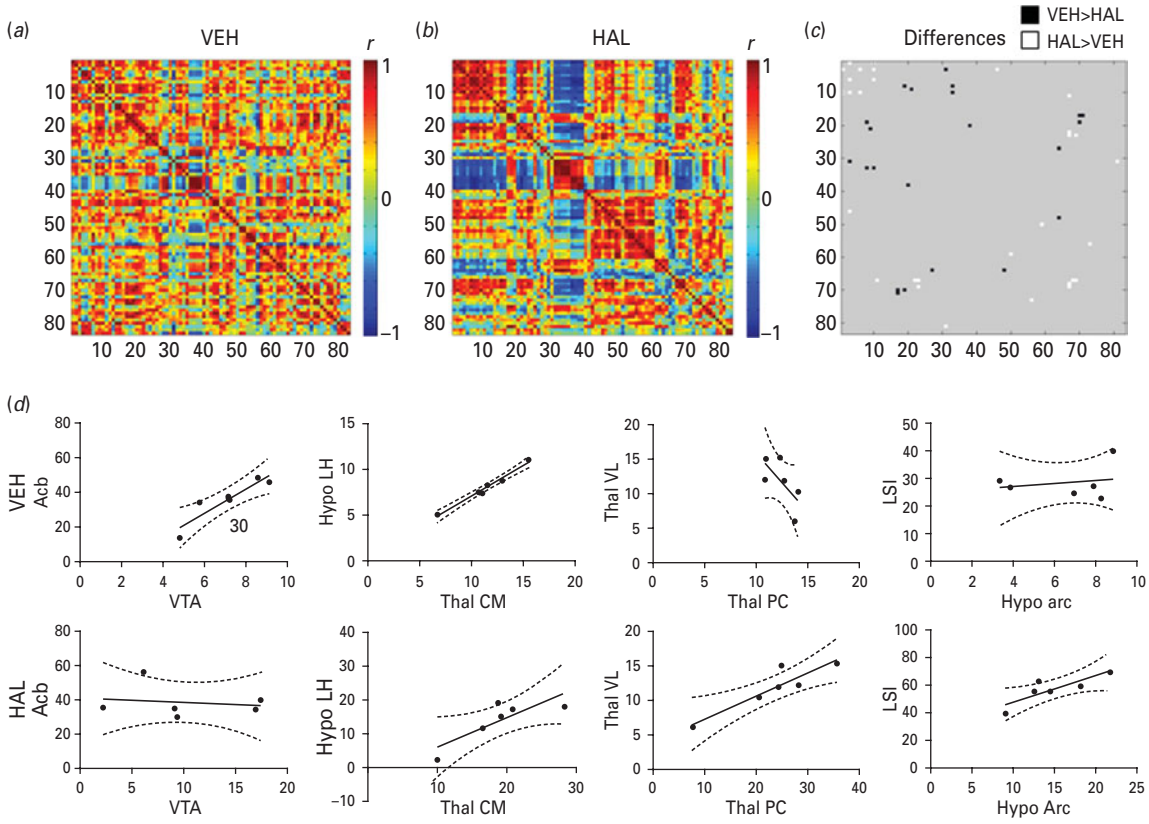

Fig. 2. Comparison of correlation matrices in vehicle (VEH)- and halop[eridol (HAL)-treated rats. Inter-region correlation matrices for VEH- (*a*) and HAL- treated (*b*) rats. Column and row numbers correspond to brain regions indicated in Table 1. Permutation testing was used to compare the two matrices; significant differences are shown graphically (*c*), and listed in Table 2. Representative correlation plots are also shown (*d*). The significance levels for comparisons was set at $p=0.05$ and were corrected with a false discovery rate of 5%.

thresholds for each network. Networks were then characterized by levels of *integration* and *segregation* across a range of possible connection density thresholds values that corresponded to retaining 50% or less of the strongest correlations. Integration in a brain network gives rise to coordinated activation of distributed neuronal populations and brain areas (Rubinov and Sporns, 2010). Network *integration* was assessed by calculating *global*

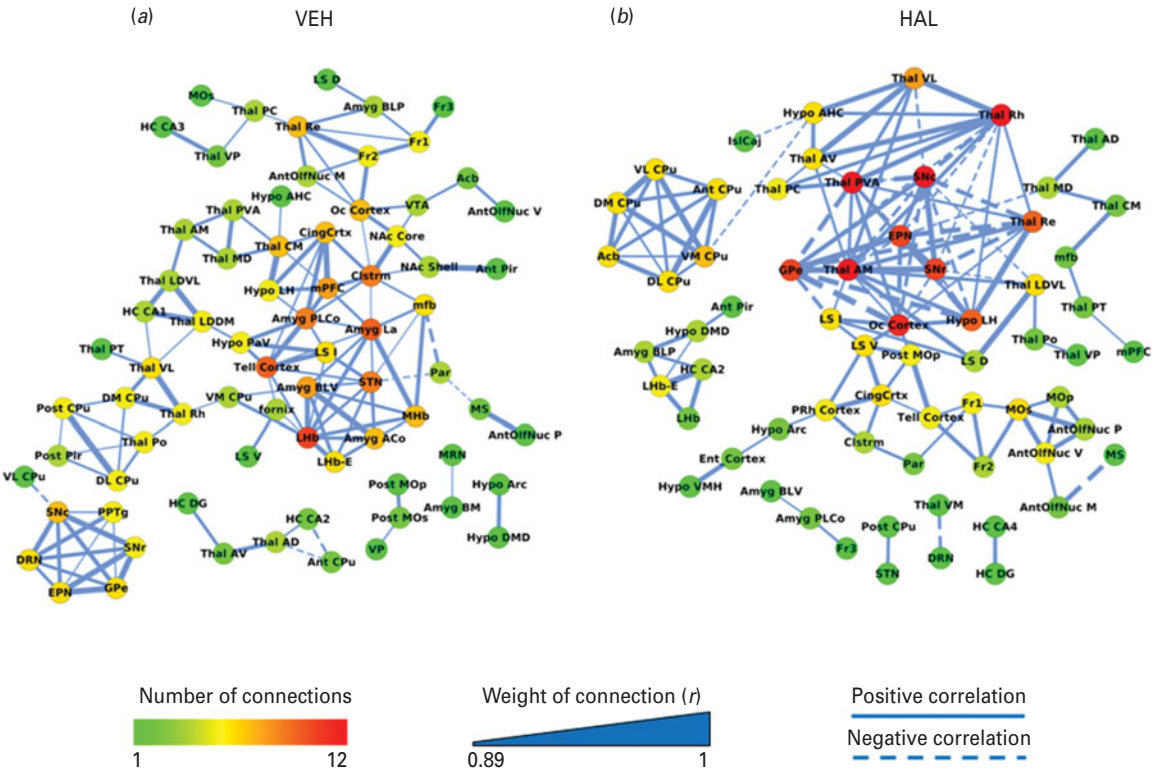

Fig. 3. Network construction and comparison. Networks were constructed by retaining the top 4% of the strongest correlations for each the haloperidol and vehicle treated groups. Nodes in the networks represent brain regions and the connections reflect super threshold correlations. The number of connections is reflected by the colour of the node, the connection strength by line thickness, and the direction of the relation, either positive or negative, by solid and dashed lines, respectively.

efficiency, defined as the average inverse shortest path length in the network (Latora and Marchiori, 2001). *Segregation* in a brain network allows for specialized processing in more densely-connected clusters (Rubinov and Sporns, 2010). Segregation was assessed by calculating the *clustering coefficient*, which is computed by dividing the number of existing connections among a node's directly connected neighbours by the number of possible connections between them (Watts and Strogatz, 1998). The mean clustering coefficient for the network is then computed as the average clustering coefficient for all of the active nodes in the network. For each network connection density, 100 random, null hypothesis networks were generated with the same number of active nodes, connections and same degree distribution. Network segregation and integration values were contrasted with averaged values from these corresponding random, control networks. Network measures and random null hypothesis networks were generated using functions from Olaf Sporns' brain connectivity toolbox (https://sites.google.com/site/bctnet/). Confidence intervals of 95% for the network measures are reported in order to determine whether network properties differ reliably between experimental networks and random, control networks. Means and confidence intervals for the network measures were derived by bootstrapping which involved resampling subjects with replacement one hundred times and recalculating the network measures.

Results

Comparison of inter-region correlation matrices

Pearson correlation matrices for all brain regions are shown in Fig. 2*a* (VEH) and 2B (HAL). Significant differences computed by permutation testing using a FDR of 5% are shown in Fig. 2*c* and are listed in Table 2. Generally, relative to VEH-treated animals, HAL-treated rats exhibited a higher degree of inter-thalamic correlation and a greater negative correlation between the caudate-putamen and thalamus. Examples of specific correlations that were different between HAL- and VEH-treated animals are shown in Fig. 2*d*. Correlation matrices generated with Spearman correlation coefficients produced very similar correlation matrices as those using Pearson correlation coefficients (data not shown).

Network properties

Connection density was found to be equivalent in HAL- and VEH-treated networks across a range of possible *r* values including the chosen threshold (Fig. 4*a*). To compare network properties, VEH and HAL networks were

Table 2. Brain regions showing significant correlations in vehicle (VEH) *vs.* haloperidol (HAL) treated brains[a]

VEH>HAL				HAL>VEH			
Region 1	Region 2	VEH *r*	HAL *r*	Region 1	Region 2	VEH *r*	HAL *r*
Thal_Rh	DM_CPu	0.96	−0.79	Ant_CPu	HC_CA2	−0.92	0.74
Thal_VL	DM_CPu	0.95	−0.80	MOp	AntOlfNuc_V	−0.68	0.95
MHb	Mfb	0.95	−0.78	Par	Amyg_La	−0.79	0.77
Oc_Cortex	Acb	0.81	−0.70	LS_D	LS_I	−0.17	0.93
Hypo_PaV	SNr	0.46	−0.85	Thal_VM	LS_D	−0.13	0.81
Thal_Rh	MHb	0.75	−0.48	LS_D	LS_V	−0.03	0.82
LHb	Fornix	0.89	−0.28	Hypo_AHC	LS_D	0.14	0.80
VTA	Acb	0.92	−0.19	Hypo_Arc	LS_I	0.23	0.84
LHb	Mfb	0.84	−0.26	Thal_PC	PRh_Cortex	0.19	0.79
Thal_PC	Ant_CPu	0.13	−0.75	Thal_PC	Thal_AM	0.30	0.80
Thal_CM	Hypo_LH	0.99	0.82	Thal_PC	Thal_VL	0.51	0.91
				Thal_PVA	Thal_PC	0.60	0.95
				Hypo_Arc	LS_D	0.38	0.72
				Thal_PVA	Thal_VL	0.79	0.94
				Thal_AM	Thal_VL	0.81	0.94

[a] The left half of the table shows region pairs for which the correlation coefficient *r* was higher in VEH- than in HAL-treated brains, the right half shows pairs for which *r* was higher in HAL- than in VEH-treated brains.

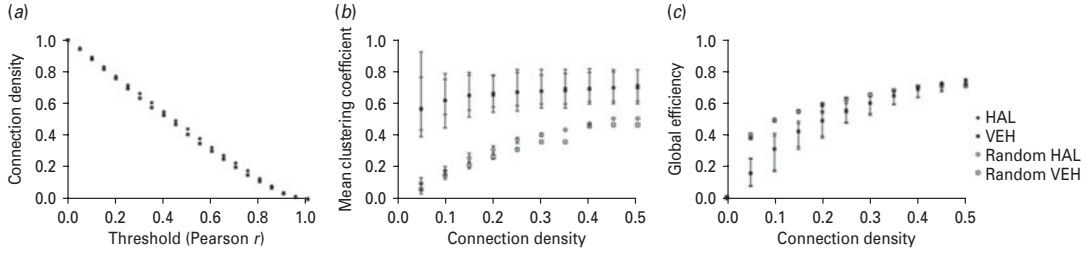

Fig. 4. Network properties across thresholds. The network connection density was dependent on the correlation threshold that was applied to the association matrices but was equivalent between the haloperidol (HAL) and vehicle (VEH) networks (*a*). Mean clustering coefficient did not differ between the HAL and VEH networks, but was greater than in the random networks at a range of connection densities (*b*). Global efficiency was equivalent between the HAL and VEH networks, and was slightly lower than, or did not differ from, that of random networks (*c*). Error bars represent 95% confidence intervals.

thresholded at a range of connection densities and matched random networks were generated. HAL and VEH networks did not differ from each other in *clustering* but did show enhanced clustering in relation to the respective random networks (Fig. 4*b*). *Global efficiency* was also equivalent in the HAL and VEH networks and was slightly lower or not different from that of random networks (Fig. 4*c*).

Network comparisons

As illustrated in Fig. 3*a*, the network for VEH-treated rats, the baseline network, was characterized by a high degree of inter-correlations between brainstem nuclei including the pedunculopontine tegmental nucleus (PPTg), substantia nigra pars compacta and pars reticulata (SNc and SNr), dorsal raphe nucleus (DR) and basal ganglia (entopeduncular nucleus (EPN) and globus pallidus (GPe)). There was also a high degree of functional connectivity between subdivisions of the caudate putamen (CPu), between midbrain nuclei (habenula and septum), the subthalamic nucleus (STN), the amygdala and several cortical regions.

In contrast, the HAL network (Fig. 2*b*) exhibited high functional connectivity between clusters of thalamic nuclei, and between basal ganglia nuclei and thalamus. Generally, the basal ganglia exhibited a much higher degree of functional connectivity following HAL treatment than in the VEH baseline network, with nearly all subdivisions of the CPu (all but the posterior subdivision) becoming highly inter-correlated. There was also a high degree of functional correlation among cortical areas.

Discussion

The objective of this study was to assess if functional relationships between brain areas change as a result of

chronic HAL treatment. To this end, inter-regional correlations were used to characterize how neural activity covaries among 83 brain regions, a measure that has been used as an indication of functional connectivity in the brain (Bullmore and Sporns, 2009; Rubinov and Sporns, 2010). By evaluating and comparing correlated activity between HAL and VEH conditions and by describing connectivity in the corresponding networks, we found that chronic HAL results in a functional network that is as segregated and integrated as the network in VEH-treated brains. We also found that that both networks display what is known as small world organization, an efficient pattern of connections that allows for most nodes in the network to reach all other nodes in a small number of steps. Finally, by comparing HAL and VEH networks we found that HAL treatment leads to altered correlated activity between the caudate-putamen and thalamus.

The caudate-putamen is the main input station of the basal ganglia, projecting through output pathways to the thalamus. Projections from the basal ganglia output nuclei to the thalamus are inhibitory and GABAergic. We observed a strong inverse correlation between activity of the CPu and thalamus following HAL treatment, which may be explained by increased strength of inhibitory input from the basal ganglia to the thalamus. A second major observation was an increased degree of inter-thalamic correlations in the HAL network. These observations may be relevant in two separate contexts related to schizophrenia and its treatment.

Evidence from different sources has implicated thalamic pathology in schizophrenia. In general, MRI studies have revealed smaller thalamic volumes in schizophrenia, as well as shape deformations suggestive of changes in thalamic regions connected to cortical areas involved in executive function and sensory integration, leading to the suggestion that schizophrenia might be a disease of disrupted thalamocortical neural networks (Cronenwett and Csernansky, 2010). However, as noted earlier, in human imaging studies it is difficult to clearly separate medication effects from changes inherent to the pathological condition itself. In this context our findings in this preclinical model may suggest that a significant portion of thalamic functional changes could be attributable to the medication itself.

Our analysis also uncovered a significant negative correlation between activity of the VTA and accumbens (Acb) following HAL-treatment. The Acb receives dopaminergic innervation from the VTA (Sesack and Grace, 2010), and this desynchronization may be related to the effects of HAL on motivation. HAL is known to impair performance on escapable shock stress and decreases motivation to obtain drugs of abuse (Carli and Samanin, 1992; McFarland and Ettenberg, 1995; Rygula et al., 2005). These effects are thought to arise from blockade of D2 receptors in the Acb, which may also be reflected by the observed decreased synchronization between VTA activity and Acb activity.

The second important context where the present results may be of interest relates to tardive dyskinetic syndromes arising after prolonged antipsychotic drug treatments (Jeste et al., 1998; Casey, 2004). Irregular activity of neurons in basal ganglia has been reported in rats and non-human primates following HAL treatment (Napier et al., 1985; Svensson, 2000; Creed et al., 2012). Pathological synchronization, or changes in functional connectivity, in the basal ganglia–thalamus–motor cortex circuit are known to be related to motor symptoms of Parkinson's disease and L-Dopa-induced dyskinesias (Damier, 2009). Similarly, changes in activity of several basal ganglia structures have been linked to motor symptoms in TD and it has been proposed that pathological changes in neuronal synchronization may be related to the development of motor symptoms in TD as well (Elkashef et al., 1994; Szymanski et al., 1996). If the observed altered connectivity between CPu and thalamus indeed reflects inhibitory input from the basal ganglia, this would be consistent with observations that surgical interventions that reduce activity of basal ganglia output nuclei to the thalamus effectively reduce HAL-induced orofacial dyskinesias (Damier et al., 2007; Thobois et al., 2008, 2011; Creed et al., 2011). In this context it is also of interest to note the change in connectivity of the subthalamic nucleus (STN), a key region involved in various forms of movement disorders including HAL-induced tardive syndromes (Creed and Nobrega, 2013). While the STN appears as a central node in the baseline VEH network, following HAL-treatment it was functionally connected only with the posterior CPu.

Recently Gass et al. (2013) reported connectivity changes using fMRI in isoflurane-anesthetized rats 20 min after a single HAL injection (1 mg/kg s.c.), where most of the observed network changes were associated with altered connectivity of the substantia nigra and, to a lesser extent, the habenula. In contrast, the present study examined the effects of prolonged rather than acute HAL and used a higher resolution functional index. Despite these important differences it is interesting that we also observed pronounced alterations in the connectivity of the substantia nigra. It would be of interest to confirm that altered thalamic connectivity observed here is indeed a feature of chronic but not acute HAL treatment.

Aside from functional implications, it is interesting that chronic HAL treatment resulted in functional networks that are as segregated and integrated as networks in vehicle treated rats, and that both networks were more segregated than matched random networks. Although, as expected, the specific architecture of the HAL and VEH networks were different, the global organization of network structure was the same. To our knowledge, this is the first study to examine alterations in functional connectivity in a model system following long-term HAL treatment. We found that a strong inverse relationship between CPu activity and thalamic activity arises after

chronic HAL treatment, and suggest that this may be a result of increased inhibitory output from the basal ganglia to thalamus. It is not possible to determine the extent to which the observed changes in functional connectivity may be related to dyskinesias, to changes in motivated behaviours and/or to the therapeutic effects of chronic HAL. However, by determining changes in functional connectivity arising from chronic HAL treatment in the absence of other interventions, the current findings provide a signature pattern that may be targeted in future efforts to discriminate between the neural basis of these different behavioural outcomes.

Acknowledgments

We thank Roger Raymond and Mustansir Diwan for excellent technical help. Supported in part by funds from the Ontario Mental Health Foundation (OMHF), Canadian Institutes of Health Research (CIHR), National Institutes of Health (NIH), the National Alliance for Research on Schizophrenia and Depression (NARSAD) and the Centre for Addiction and Mental Health Foundation (Kimel Family). A.L.W. was the recipient of an OMHF Postdoctoral Fellowship and M.C.C. the recipient of a CIHR Doctoral Award. A.N.V. was the recipient of a Keorner New Scientist Award and a Paul E Garfinkel New Investigator Catalyst Award.

Statement of Interest

None.

References

Benes FM, Paskevich PA, Davidson J, Domesick VB (1985a) The effects of haloperidol on synaptic patterns in the rat striatum. Brain Res 329:265–273.

Benes FM, Paskevich PA, Davidson J, Domesick VB (1985b) Synaptic rearrangements in medial prefrontal cortex of haloperidol-treated rats. Brain Res 348:15–20.

Benjamini Y, Rochberg Y (1995) Controlling the false discovery rate: a practical and powerful approach to multiple testing. J R Stat Soc B 57:289–300.

Bullmore E, Sporns O (2009) Complex brain networks: graph theoretical analysis of structural and functional systems. Nat Rev Neurosci 10:186–198.

Carli M, Samanin R (1992) Serotonin2 receptor agonists and serotonergic anorectic drugs affect rats' performance differently in a five-choice serial reaction time task. Psychopharmacology (Berl) 106:228–234.

Casey DE (2004) Pathophysiology of antipsychotic drug-induced movement disorders. J Clin Psychiatry 65 (Suppl. 9):25–28.

Chakos MH, Shirakawa O, Lieberman J, Lee H, Bilder R, Tamminga CA (1998) Striatal enlargement in rats chronically treated with neuroleptic. Biol Psychiatry 44:675–684.

Cline MS et al. (2007) Integration of biological networks and gene expression data using Cytoscape. Nat Protoc 2:2366–2382.

Creed M, Hamani C, Nobrega JN (2011) Deep brain stimulation of the subthalamic or entopeduncular nucleus attenuates vacuous chewing movements in a rodent model of tardive dyskinesia. Eur Neuropsychopharmacol 21:393–400.

Creed MC, Nobrega JN (2013) Neurobiological basis of dyskinetic effects induced by antipsychotics: the contribution of animal models. Curr Med Chem 20:389–396.

Creed MC, Hamani C, Nobrega JN (2012) Early gene mapping after deep brain stimulation in a rat model of tardive dyskinesia: comparison with transient local inactivation. Eur Neuropsychopharmacol 22:506–517.

Cronenwett WJ, Csernansky J (2010) Thalamic pathology in schizophrenia. Curr Top Behav Neurosci 4:509–528.

Damier P (2009) Drug-induced dyskinesias. Curr Opin Neurol 22:394–399.

Damier P, Thobois S, Witjas T, Cuny E, Derost P, Raoul S et al. (2007) Bilateral deep brain stimulation of the globus pallidus to treat tardive dyskinesia. Arch Gen Psychiatry 64:170–176.

Dong J, Horvath S (2007) Understanding network concepts in modules. BMC Syst Biol 1:24.

Eastwood SL, Heffernan J, Harrison PJ (1997) Chronic haloperidol treatment differentially affects the expression of synaptic and neuronal plasticity-associated genes. Mol Psychiatry 2:322–329.

Eastwood SL, Cairns NJ, Harrison PJ (2000) Synaptophysin gene expression in schizophrenia. Investigation of synaptic pathology in the cerebral cortex. Br J Psychiatry 176:236–242.

Ebdrup BH, Norbak H, Borgwardt S, Glenthoj B (2013) Volumetric changes in the basal ganglia after antipsychotic monotherapy: a systematic review. Curr Med Chem 20:438–447.

Elkashef AM, Egan MF, Frank JA, Hyde TM, Lewis BK, Wyatt RJ (1994) Basal ganglia iron in tardive dyskinesia: an MRI study. Biol Psychiatry 35:16–21.

Farivar R, Zangenehpour S, Chaudhuri A (2004) Cellular-resolution activity mapping of the brain using immediate-early gene expression. Front Biosci 9:104–109.

Gass N, Schwarz AJ, Sartorius A, Cleppien D, Zheng L, Schenker E, Risterucci C, Meyer-Lindenberg A, Weber-Faht W (2013) Haloperidol modulates midbrain-prefrontal functional connectivity in the rat brain. Eur Neuropsychopharmacol 10:1310–1319.

Genovese CR, Lazar NA, Nichols T (2002) Thresholding of statistical maps in functional neuroimaging using the false discovery rate. Neuroimage 15:870–878.

Harrison PJ (1999) The neuropathological effects of antipsychotic drugs. Schizophr Res 40:87–99.

Jeste DV, Lohr JB, Eastham JH, Rockwell E, Caligiuri MP (1998) Adverse neurobiological effects of long-term use of neuroleptics: human and animal studies. J Psychiatr Res 32:201–214.

Kelley JJ, Gao XM, Tamminga CA, Roberts RC (1997) The effect of chronic haloperidol treatment on dendritic spines in the rat striatum. Exp Neurol 146:471–478.

Konradi C, Heckers S (2001) Antipsychotic drugs and neuroplasticity: insights into the treatment and neurobiology of schizophrenia. Biol Psychiatry 50:729–742.

Latora V, Marchiori M (2001) Efficient behavior of small-world networks. Phys Rev Lett 87:198701.

McFarland K, Ettenberg A (1995) Haloperidol differentially affects reinforcement and motivational processes in rats running an alley for intravenous heroin. Psychopharmacology (Berl) 122:346–350.

Napier TC, Coyle S, Breese GR (1985) Ontogeny of striatal unit activity and effects of single or repeated haloperidol administration in rats. Brain Res 333:35–44.

Paxinos G, Watson C (1986) The rat brain in stereotaxic coordinates. New York: Academic Press.

Pizzolato G, Soncrant TT, Holloway HW, Rapoport SI (1985a) Reduced metabolic response of the aged rat brain to haloperidol. J Neurosci 5:2831–2838.

Pizzolato G, Soncrant TT, Larson DM, Rapoport SI (1985b) Reduced metabolic response of the rat brain to haloperidol after chronic treatment. Brain Res 337:1–9.

Roberts RC, Lapidus B (2003) Ultrastructural correlates of haloperidol-induced oral dyskinesias in rats: a study of unlabelled and enkephalin-labelled striatal terminals. J Neural Transm 110:961–975.

Roberts RC, Gaither LA, Gao XM, Kashyap SM, Tamminga CA (1995) Ultrastructural correlates of haloperidol-induced oral dyskinesias in rat striatum. Synapse 20:234–243.

Roder CH, Dieleman S, van der Veen FM, Linden D (2013) Systematic review of the influence of antipsychotics on the blood oxygenation level-dependent signal of functional magnetic resonance imaging. Curr Med Chem 20:448–461.

Rubinov M, Sporns O (2010) Complex network measures of brain connectivity: uses and interpretations. Neuroimage 52:1059–1069.

Rygula R, Abumaria N, Flugge G, Fuchs E, Ruther E, Havemann-Reinecke U (2005) Anhedonia and motivational deficits in rats: impact of chronic social stress. Behav Brain Res 162:127–134.

Sesack SR, Grace AA (2010) Cortico-Basal Ganglia reward network: microcircuitry. Neuropsychopharmacology 35:27–47.

Sun YJ, Suzuki M, Kurachi T, Murata M, Kurachi M (1998) Expression of Fos protein in the limbic regions of the rat following haloperidol decanoate. Brain Res 791:125–136.

Svensson TH (2000) Dysfunctional brain dopamine systems induced by psychotomimetic NMDA-receptor antagonists and the effects of antipsychotic drugs. Brain Res Brain Res Rev 31:320–329.

Szymanski S, Gur RC, Gallacher F, Mozley LH, Gur RE (1996) Vulnerability to tardive dyskinesia development in schizophrenia: an FDG-PET study of cerebral metabolism. Neuropsychopharmacol 15:567–575.

Teo JT, Edwards MJ, Bhatia K (2012) Tardive dyskinesia is caused by maladaptive synaptic plasticity: a hypothesis. Mov Disord 27:1205–1215.

Thobois S, Ballanger B, Xie-Brustolin J, Damier P, Durif F, Azulay JP et al. (2008) Globus pallidus stimulation reduces frontal hyperactivity in tardive dystonia. J Cereb Blood Flow Metab 28:1127–1138.

Thobois S, Poisson A, Damier P (2011) Surgery for tardive dyskinesia. Int Rev Neurobiol 98:289–296.

Turrone P, Remington G, Nobrega JN (2002) The vacuous chewing movement (VCM) model of tardive dyskinesia revisited: is there a relationship to dopamine D(2) receptor occupancy? Neurosci Biobehav Rev 26:361–380.

Vernon AC, Natesan S, Modo M, Kapur S (2011) Effect of chronic antipsychotic treatment on brain structure: a serial magnetic resonance imaging study with *ex vivo* and postmortem confirmation. Biol Psychiatry 69:936–944.

Vernon AC, Natesan S, Crum WR, Cooper JD, Modo M, Williams SC et al. (2012) Contrasting effects of haloperidol and lithium on rodent brain structure: a magnetic resonance imaging study with postmortem confirmation. Biol Psychiatry 71:855–863.

Watts DJ, Strogatz SH (1998) Collective dynamics of 'small-world' networks. Nature 393:440–442.

Wheeler AL, Teixeira CM, Wang AH, Xiong X, Kovacevic N, Lerch JP et al. (2013) Identification of a functional connectome for long-term fear memory in mice. PLoS Comput Biol 9: e1002853.